

UC Davis

UC Davis Previously Published Works

Title

White matter microstructural abnormalities in girls with chromosome 22q11.2 deletion syndrome, Fragile X or Turner syndrome as evidenced by diffusion tensor imaging

Permalink

<https://escholarship.org/uc/item/4t20m347>

Authors

Villalon-Reina, Julio
Jahanshad, Neda
Beaton, Elliott
[et al.](#)

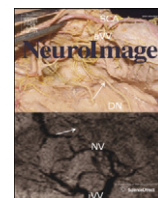
Publication Date

2013-11-01

DOI

10.1016/j.neuroimage.2013.04.028

Peer reviewed



White matter microstructural abnormalities in girls with chromosome 22q11.2 deletion syndrome, Fragile X or Turner syndrome as evidenced by diffusion tensor imaging

Julio Villalon-Reina^a, Neda Jahanshad^a, Elliott Beaton^e, Arthur W. Toga^b, Paul M. Thompson^{a,*}, Tony J. Simon^{c,d}

^a Imaging Genetics Center, Laboratory of Neuro Imaging, Dept. of Neurology, University of California Los Angeles, School of Medicine, Los Angeles, CA 90095, USA

^b Laboratory of Neuro Imaging, Dept. of Neurology, University of California Los Angeles, School of Medicine, Los Angeles, CA 90095, USA

^c Dept. of Psychiatry and Behavioral Sciences, University of California, Davis, Sacramento, CA, 95618, USA

^d MIND Institute, Dept. of Psychiatry and Behavioral Sciences, University of California, Davis, Sacramento, CA, 95618, USA

^e Stress, Cognition, and Affective Neuroscience Laboratory, Department of Psychology, University of New Orleans, New Orleans, LA, 70148

ARTICLE INFO

Article history:

Accepted 10 April 2013

Available online 18 April 2013

Keywords:

Diffusion tensor imaging

Genetic diseases

Neurodevelopmental diseases

Connectivity

ABSTRACT

Children with chromosome 22q11.2 deletion syndrome (22q11.2DS), Fragile X syndrome (FXS), or Turner syndrome (TS) are considered to belong to distinct genetic groups, as each disorder is caused by separate genetic alterations. Even so, they have similar cognitive and behavioral dysfunctions, particularly in visuospatial and numerical abilities. To assess evidence for common underlying neural microstructural alterations, we set out to determine whether these groups have partially overlapping white matter abnormalities, relative to typically developing controls. We scanned 101 female children between 7 and 14 years old: 25 with 22q11.2DS, 18 with FXS, 17 with TS, and 41 aged-matched controls using diffusion tensor imaging (DTI). Anisotropy and diffusivity measures were calculated and all brain scans were nonlinearly aligned to population and site-specific templates. We performed voxel-based statistical comparisons of the DTI-derived metrics between each disease group and the controls, while adjusting for age. Girls with 22q11.2DS showed lower fractional anisotropy (FA) than controls in the association fibers of the superior and inferior longitudinal fasciculi, the splenium of the corpus callosum, and the corticospinal tract. FA was abnormally lower in girls with FXS in the posterior limbs of the internal capsule, posterior thalami, and precentral gyrus. Girls with TS had lower FA in the inferior longitudinal fasciculus, right internal capsule and left cerebellar peduncle. Partially overlapping neurodevelopmental anomalies were detected in all three neurogenetic disorders. Altered white matter integrity in the superior and inferior longitudinal fasciculi and thalamic to frontal tracts may contribute to the behavioral characteristics of all of these disorders.

© 2013 Elsevier Inc. All rights reserved.

Introduction

Children with chromosome 22q11.2 deletion syndrome (22q11.2DS), Fragile X syndrome (FXS), or Turner syndrome (TS) are considered to belong to genetically distinct groups, as each disorder has a specific, apparently nonoverlapping, genetic cause. Yet, many of the cognitive differences manifested by affected children are common across the three disorders. Some of the major commonalities involve impairments in visuospatial and numerical cognitive competence (Simon, 2007, 2011; Simon et al., 2008a). It is therefore reasonable to hypothesize that there may be shared patterns of altered brain development that lead to these cognitive and behavioral changes.

22q11.2DS is the most common microdeletion syndrome with a prevalence of 1 in 4000–7000 live births (Burn and Goodship, 1996). In around 90% of cases (Bittel et al., 2009), the deletion on the long (*q*) arm of chromosome 22 is 3 Mb in size and encompasses approximately 30 genes. Children with 22q11.2DS often show mild intellectual impairment (IQ is typically in the 70–80s) and, in most, non-verbal skills are affected more than verbal skills (De Smedt et al., 2007; Wang et al., 2000). Other cognitive impairments involve disrupted visuospatial attention and working memory, and impaired numerical ability (Bearden et al., 2001; Simon et al., 2005b, 2008a,b). Individuals with 22q11.2DS are at increased risk of developing psychiatric disorders, in particular schizophrenia and schizoaffective disorder (Gothelf et al., 2007a,b; Green et al., 2009; Stoddard et al., 2010). Differences in brain morphology with respect to healthy subjects include volumetric reductions in brain regions such as the hippocampus, thalamus and neocortex. There is also reduced cortical thickness and a range of midline anomalies including enlarged lateral ventricles, more prominent *cavum septum pellucidum*, and callosal differences (Karayiorgou et al.,

* Corresponding author at: Imaging Genetics Center, Laboratory of Neuro Imaging, UCLA School of Medicine, 635 Charles Young Drive, Los Angeles, CA 90095, USA. Fax: +1 310 206 5518.

E-mail address: thompson@loni.ucla.edu (P.M. Thompson).

2010). Animal models and human neuropathological studies of 22q11.2DS have shown that the main developmental disruption occurs during neuronal migration (Kiehl et al., 2009; Meechan et al., 2009). Other radiological reports in these subjects have included heterotopia and polymicrogyria (Robin et al., 2006). Disrupted migration supports the idea that neuronal connectivity may develop abnormally, making it a natural target of study using diffusion tensor imaging.

FXS is an X-linked dominant neurodevelopmental disorder caused by the silencing of the *FMR1* (Fragile X Mental Retardation 1 gene), due to an expansion of a CGG repeat in the 5'-untranslated region. A "full mutation" exists when there are more than 200 triplet repeats within the gene. Numerous studies estimate FXS prevalence at 1 in 4000 male births and 1 in 8000 female births for individuals with the "full mutation" (Crawford et al., 1999). The mutation extinguishes the expression of the *FMR1* gene product, namely Fragile X Mental Retardation Protein (FMRP) (Oberle et al., 1991; Verkerk et al., 1991). FMRP is found mainly in the perikaryon, dendrites and synapses. It is an mRNA binding protein, transporting mRNAs from the transcription site to the dendrites in response to synaptic stimuli. Low levels of the protein affect development of synapses and dendrites, and disrupt axon directionality and coherence (Galvez and Greenough, 2005). These abnormalities in neuronal development have a phenotypic expression in brain structure that has been documented in brain imaging studies (Reiss et al., 1995a; Kates et al., 1997; Lee et al., 2007; Eliez et al., 2001a). In addition to this, subjects affected with FXS also present weaknesses in visuospatial working memory and perception, mental manipulation of visual-spatial relationships among objects, attention and visual-motor coordination (Cornish et al., 1999; Farzin and Rivera, 2010; Freund and Reiss, 1991; Kogan et al., 2004; Mazzocco et al., 2006; Murphy et al., 2006; Scerif et al., 2004, 2007) as well as problems in arithmetic reasoning and computation, similar to those in 22q11.2DS (Murphy et al., 1993).

TS occurs in approximately 1 in 2000 live female births (Lippe, 1991). These individuals lack a complete copy or a portion of one of the X chromosomes. This deletion causes a myriad of physical characteristics and medical problems, particularly cardiovascular malformations, kidney malformations and nonfunctional ovaries. Females with TS do not have a global cognitive impairment but they do have a particular cognitive phenotype, which mainly consists of difficulty with visuospatial tasks, visuomotor control and, as with individuals with 22q11.2DS or FXS, impairments in numerical ability (Beaton et al., 2010; Bruandeta et al., 2004; Hart et al., 2006; Kesler et al., 2004; Mazzocco et al., 2006; Murphy et al., 2006; Reiss et al., 1995b; Romans et al., 1998; Ross et al., 2000; Rovet and Netley, 1980; Rovet and Ireland, 1994; Silbert et al., 1977; Temple and Carney, 1995). The cognitive characteristics also vary across subjects affected by TS. This is explained by multiple factors that have been proven to affect brain development and function in TS subjects: (1) mosaic or non-mosaic karyotype (Kesler et al., 2003); (2) X-linked imprinting (Bishop et al., 2000); (3) lack of endogenous estrogenic influence on brain development (Arnold and Gorski, 1984); and, (4) treatment based on hormonal substitution (estrogens, androgens and growth hormones) (Nilsson et al., 1996). Imaging studies show decreased regional brain volumes in the parietal and occipital lobes, hippocampus, caudate nucleus, and thalamus (Brown et al., 2002, 2004; Murphy et al., 1993; Reiss et al., 1995b).

Neuroimaging approaches may be used to uncover common patterns of functional and anatomical differences in children with these disorders to help relate genetic variations to brain organization and behavior. This is called a *behavioral neurogenetics* approach (Reiss and Dant, 2003). To identify possible common mechanisms and pathways involved in the etiology of these three disorders, we used diffusion tensor imaging (DTI) to map the 3D profile of white matter abnormalities in children with 22q11.2DS, FXS, and TS compared to typically developing (TD) children. DTI is a variant of magnetic resonance imaging (MRI) that enables the study of the white matter microstructure, including tracts. These tracts are formed by coherent bundles of axons, in which water diffusion is hindered by cell membranes and the myelin sheaths

that surround them. DTI visualizes the directionality of water diffusion, which is greater along the axis of the axons than perpendicular to them.

Here, we set out to determine whether specific patterns of abnormal white matter microstructure are found within each of the genetic disorders, and whether common patterns of neuroanatomical abnormalities can be observed within the three disorders. In terms of cognition, there are two impairments shared by these 3 neurogenetic syndromes – impairments in visuospatial processing and numerical (including arithmetic) ability. Numerical and arithmetic abilities are thought to share some neural/cognitive processes with visuospatial tasks (representation of a mental number line, alignment of digits in calculation, borrowing/carrying concepts). Since numerical abilities develop later than visuospatial abilities it has become widely accepted that the latter is constructed out of, or at least depends heavily on, the former (Hubbard et al., 2005; Simon, 1997, 2011; Walsh, 2003). Visual processing is thought to involve two "streams" of information processing: the dorsal "where" stream (encoding information on spatial position) and the ventral "what" stream (encoding information on shape recognition and differentiation). The three syndromes analyzed here may all involve dorsal visual processing stream impairments (Bearden et al., 2001; Braddick et al., 2003; Farzin et al., 2008; Hoefft et al., 2007a; Kesler et al., 2004). At least one review reports common neural differences (Walter et al., 2009) – primarily abnormal structure and function of the parietal lobe (important for visuospatial and arithmetic tasks) and the superior longitudinal fasciculus (SLF).

Some initial DTI studies on 22q11.2DS report altered white matter anisotropy in occipital, parietal and frontal regions (Barnea-Goraly et al., 2003b; Simon et al., 2005a, 2008b). DTI analysis has revealed lower anisotropy in frontal-striatal and parietal sensorimotor tracts along the *corona radiata* and *centrum semiovale* in FXS (Barnea-Goraly et al., 2003a). And in TS, DTI studies reveal lower anisotropy in fronto-parietal white matter, prefrontal cortex close to the caudate, orbitofrontal region, and in bilateral internal capsules and higher FA in the temporoparietal pathways (Holzapfel et al., 2006). We hypothesized that common developmental abnormalities would be found within the white matter structure across all three disorders, compared to controls, especially in areas that carry long association fibers. Long association fibers such as the SLF, the inferior longitudinal fasciculus (ILF) and the inferior fronto-occipital fasciculus (IFO) connect lobes within the hemispheres. They transfer information from anterior to posterior regions of the brain or vice versa. These areas comprise the anterior branch of the internal capsule, the external capsule, and non-specific white matter in the temporal, parietal and frontal lobes.

We hypothesized that common developmental abnormalities would be found within the white matter structure between all three disorders when compared to controls, especially in those areas where long association fibers travel. Long association fibers such as the SLF, the inferior longitudinal fasciculus (ILF) and the inferior fronto-occipital fasciculus (IFO) are long association fibers that connect lobes within the hemispheres transferring information from anterior to posterior portions of the brain or vice versa. Those areas comprise the anterior branch of the internal capsule, the external capsule, and non-specific white matter in the temporal, parietal and frontal lobes.

Methods

Participants and scanning protocol

Quality control of the data was done to eliminate scans that did not adhere to our protocol suffered from severe motion artifacts. Scans were collected at two locations (Tables 1 and 2). One group included the children with 22q11.2DS, FXS and corresponding age-matched TD controls (total 57 children) scanned at the University of California Davis Medical Center, in Davis, California (UCDMC). This group included 20 TD girls ranging in age from 7 to 14 years (mean: 10.17 ± 2.28 years), 19 girls with 22q11.2DS, ranging in age from 7

Table 1

Detailed description of the three groups of subjects scanned at the University of California Davis Medical Center (UCDMC). The scanning protocol of the diffusion MRI at this site is also specified.

Site	University of California Davis Medical Center (UCDMC), Davis, California		
Disease group	22q11.2 deletion syndrome (22q11.2DS)	Fragile X syndrome (FXS)	Typically developing (TD1)
N subjects	19	18	20
Age (years)	7–14 years (10.75 ± 1.87)	7–14 years (11.01 ± 2.12)	7–14 years (10.17 ± 2.28)
Scanner type	3 T Siemens MAGNETOM Trio (Siemens Medical Solutions, Erlangen, Germany)		
Sequence type	Single shot EPI		
Parameters	TE/TR = 99/6700 ms		
Resolution	1.72 × 1.75 × 3 mm ³		
Slices	40		
FOV	220 × 220 mm ²		
Gradients	1 b ₀ /12 b = 1000 s/mm ²		
Acquisitions	1		

to 14 years (mean: 10.75 ± 1.87), and 18 girls with FXS, ranging in age from 7 to 14 years (mean: 11.01 ± 2.12 years). Separate groups of children were scanned at the Thomas Jefferson University (TJU) in Philadelphia, PA including 19 TD females ranging in age from 6 to 14 years (mean: 10.6 ± 2.2) as well as 15 girls with TS from 7 to 13 years of age (mean: 10.56 ± 2.67 years). All the TS girls were nonmosaic (45,X karyotype) and none of them was being treated with estrogen at the moment of the image acquisition. We only analyzed girls for 22q11.2DS and FXS since we wanted to exclude gender as a confounding factor between TS (affected individuals are genetically determined to be females) and these diseases.

Scans from UCDMC were acquired on a 3.0-Tesla Siemens MAGNETOM Trio scanner (Siemens Medical Solutions, Erlangen, Germany) and consisted of a DTI sequence based on single-shot echo planar imaging, with the following parameters: field of view (FOV) = 22 cm × 22 cm, matrix size = 128 × 128, TE/TR = 99/6700 ms, 40 axial slices, slice thickness 3 mm, and in-plane resolution of 1.72 × 1.72 mm². We acquired 13 volumes per subject: one with no diffusion sensitization and 12 diffusion-weighted images (with a diffusion weighting set to b = 1000 s/mm²), with gradient directions uniformly distributed on the unit hemisphere, for unbiased angular sampling of diffusion. T1 weighted structural images were also acquired for all of the 57 subjects of this group with the following parameters: MPRAGE, TE = 4.82 ms, TR = 2170 ms IT = 1100 ms, FOV = 25.6 cm × 25.6 cm, in-plane resolution of 256 × 256 with 192 slices, slice thickness of 1.00 mm.

The scans at TJU were collected using a Philips 3.0-Tesla whole body clinical MRI system (Achieva, Philips Medical Systems, Best,

Table 2

Description of the two groups of subjects scanned at the Thomas Jefferson University. The scanning protocol of the diffusion MRI at this site is specified as well.

Site	Thomas Jefferson University (TJU) in Philadelphia, Pennsylvania	
Disease group	Turner syndrome (TS)	Typically developing (TD2)
N subjects	15	19
Age (years)	7–14 years (10.56 ± 2.67)	7–14 years (10.6 ± 2.2)
Scanner type	3 T Philips Achieva (Philips Medical Systems, Best, The Netherlands)	
Sequence type	Single Shot EPI	
Parameters	TE/TR = 99/6700 ms	
Resolution	1.19 × 1.19 × 3 mm ³	
Slices	40	
FOV	152 × 152 mm ²	
Gradients	1 b ₀ /16 b = 1000 s/mm ²	
Acquisitions	4	

The Netherlands) equipped with a Quasar Dual high performance gradient system. Subjects scanned included the individuals with Turner syndrome with their corresponding typically developing controls. The acquisition consisted of a single-shot echo planar imaging and SENSE (sensitivity encoding) sequence to reduce scan time (TE/TR 99/6700 ms, 15.2 cm FOV, 128 × 128). Each 3D volume consisted of 40 axial slices (1.19 mm × 1.19 mm × 3 mm). The imaging protocol included a single non-diffusion-weighted (b = 0 s/mm²) reference image followed by 16 diffusion-weighted images with different gradient directions, with a diffusion weighting of b = 1000 s/mm², for a total of 17 volumes. The gradient directions were distributed uniformly on the unit hemisphere, for unbiased angular sampling of diffusion. Additionally, each subject had four full acquisitions of the 17 volumes. T1 weighted structural images were acquired with an MPRAGE protocol for the 34 subjects of this group. The parameters were: TE = 3.2 ms, TR = 6 ms, FOV = 25.6 cm × 25.6 cm, in-plane resolution = 256 × 256 with 160 slices, slice thickness of 1 mm.

Once scanning was finished, quality control of the data was done to eliminate scans that did not adhere to our protocol or that suffered from severe motion artifacts. Comparisons were made only between groups imaged on the same scanner, to avoid confounding effects of scanning site. The methods described below, i.e. DTI preprocessing, anisotropy and diffusivity computation, template creation and registration, and statistical analysis, were done separately for each of the two scanning groups specified in Tables 1 and 2. We analyzed five groups of participants – 3 of them scanned at UCDMC: 19 girls with 22q11.2DS, 18 girls with FXS and 20 typically developing girls; and 2 of them scanned at TJU: 15 girls with TS and 19 typically developing girls. The 22q11.2DS and the FXS groups were compared to the 20 typically developing girls at UCDMC. We refer to the typically developing group from this site as TD1 below. The TS group and the 19 typically developing girls from TJU were also compared in the statistical analysis; below, we use TD2 to refer to the typically developing group scanned at TJU.

Structural T1-images preprocessing

We used the robust, learning-based brain extraction system (ROBEX) to skullstrip the brain T1-weighted images (Iglesias et al., 2011). After automatically delineating the brains, we had an expert delineator manually examine each of these to correct for any inconsistencies, using BrainSuite's visual interface (<http://users.ionu.ucla.edu/~shattuck/brainsuite>). We then corrected the skull-stripped T1 images for intensity non-uniformities using N3 (<http://www.bic.mni.mcgill.ca/ServicesSoftware/HomePage>). Then, by using FSL's FLIRT tool (Jenkinson and Smith, 2001), we linearly aligned, with 6 degrees of freedom, the skull-stripped T1 images for each child to the NIH pediatric atlas (NIHPD) (<http://www.bic.mni.mcgill.ca/ServicesAtlases/NIHPD-obj1>) (Fonov et al., 2011) that was previously downsampled to a 110 × 110 × 110 resolution. We used the asymmetric, T1 version of the NIHPD atlas, age range 7.5–13.5 years old (pre- to mid puberty), based on 162 subjects.

DTI preprocessing

We automatically removed non-brain regions from the b₀ (non-diffusion weighted) images using FSL's BET (Smith, 2002) (<http://fsl.fmrib.ox.ac.uk/fsl/>) then manually refined the brain extraction. The 4 scans of each child's data acquired at TJU were co-registered into a single volume for further processing. Raw diffusion weighted images (DWIs) were corrected for eddy current distortions using FSL's "eddy_correct" method.

Next, the b₀ image of each subject was linearly aligned to the corresponding T1 structural image that was previously aligned to the 110 × 110 × 110 NIHPD atlas using 9 degrees of freedom so that both the T1 and DWI images were in the same space, and in performing

this alignment, generated subject-specific transformation matrices. These transformation matrices were then applied to the rest of the subjects' volumes and were used to rotate the original scanner gradient vectors.

In order to adjust for any echo planar imaging (EPI)-induced susceptibility artifacts, we performed a 3D non-linear inverse-consistent elastic intensity-based warping technique with a mutual information cost function (Leow et al., 2005) of the b_0 image (previously linearly aligned to the T1 structural image) to each subject's T1 image. The transformation derived from this registration was then applied to all of the DWI volumes.

Computing anisotropy and diffusivity

Once we rotated the original gradient vectors using the rotation matrix from the linear transformation to the T1 structural image and the DWI volumes that were corrected for EPI-induced distortions, we computed diffusion tensors and derived scalar measures, using FSL. Fractional anisotropy (FA) is the most common measure of fiber integrity derived from DTI. It represents at a microstructural level the integrity of myelinated neuronal fiber tracts as well as fiber diameter and density. At a macrostructural level, it represents the fiber-tract coherence. We compared FA values at each voxel between the 3 diagnostic groups and the typically developing control children. FA was calculated from the tensor eigenvalues ($\lambda_1, \lambda_2, \lambda_3$), according to the standard formula:

$$FA = \sqrt{\frac{3}{2} \frac{\sqrt{(\lambda_1 - \langle \lambda \rangle)^2 + (\lambda_2 - \langle \lambda \rangle)^2 + (\lambda_3 - \langle \lambda \rangle)^2}}{\sqrt{(\lambda_1^2 + \lambda_2^2 + \lambda_3^2)}}} \in [0, 1]$$

$$\langle \lambda \rangle = \frac{\lambda_1 + \lambda_2 + \lambda_3}{3}$$

where $\langle \lambda \rangle$ is the mean diffusivity. Mean diffusivity (MD) is an overall summary measure of the diffusion in all directions, in a voxel or region. It can be interpreted as the mean displacement of the water molecules within the voxel and also characterizes the overall presence of obstacles to diffusion.

Axial diffusivity (AD) represents the principal eigenvalue (λ_1) of the diffusion tensor – that is, the diffusion along the dominant direction within the voxel (i.e., along the dominant fiber). AD has been associated with axonal integrity (Assaf et al., 2008). Radial diffusivity (RD) characterizes the other two eigenvalues of the tensor (λ_2, λ_3) – measuring diffusivity along the two axes orthogonal to the principal one. RD is defined as:

$$(\lambda_2 + \lambda_3)/2.$$

It has been shown that RD is decreased when there is myelin loss (Assaf et al., 2008; Tournier et al., 2011) and is also associated with myelin content in the white matter, although lower RD values do not necessarily indicate demyelination. We hypothesized that we might find higher MD, AD, and RD in atypically developing girls compared to TD girls.

Template creation and registration

As we analyzed data from two different scanning locations, we kept the two data sets (acquired on the different scanners) separate for processing and analysis. In particular, starting from this point of the analysis; a minimal deformation template (MDT) is created for each group and all subjects are registered to each group's MDT.

First we created an FA-based minimal deformation template (MDT) – a template image used for registration that represents common anatomical features for a group of participants. From the set of scans acquired at UCDMC (22q11.2DS, FXS and TD1), we took the FA maps of

all the typically developing girls (TD1 group) to create the MDT, which we will call MDT-1. In the same way, all the FA maps from the typically developing girls scanned at TJU (TD2) were used to create their corresponding MDT, which we will call MDT-2.

To compute both MDTs (MDT-1 and MDT-2), the first step was to create an affine average template. We used 12-parameter AIR to register images affinely (Woods et al., 1998). For group-wise registration, $N \times (N-1)$ transformations were computed and composed using the AIR 'reconcile' tool to bring all images into a common 12-parameter space. The second step was to create a non-linear average. For this, all individual FA maps were non-linearly registered to the affine average template (mean of the affinely aligned images) using a non-linear inverse-consistent fluid intensity-based registration algorithm (Leow et al., 2007). The non-linear average template was computed as a voxel-wise average of the intensities of the FA maps that had been non-linearly registered to the affine average template. Finally, we created the MDT by applying the inverse of the average deformation field to the mean of nonlinearly registered images.

FA maps of all children with each of the three genetic disorders and all typical developing controls were registered to their corresponding FA-based MDT using a 3D non-linear inverse-consistent elastic intensity-based warping technique with a mutual information cost function (Leow et al., 2005). Thus, 22q11.2DS, FXS and TD1 groups were registered to MDT-1, and TS and TD2 groups were registered to MDT-2.

To better align white matter regions of interest, the FA-MDTs (MDT-1, and MDT-2) and all whole-brain registered FA maps from each individual subject were thresholded at $FA > 0.2$ to exclude contributions from non-white matter. Thresholded FA maps were re-registered to the corresponding thresholded MDT. Additionally, we applied the deformation fields computed from the first round registration (whole FA volume to whole MDT) and last round registration (from the thresholded-FA to the thresholded MDT) to each subject's previously computed mean, axial and radial diffusivity maps.

Tissue specific smoothing compensation

We implemented the tissue-specific-smoothing compensation method (T-SPOON) as described in Lee et al. (2009). Once each subject's FA map was non-linearly registered to the minimal deformation template, we thresholded these FA maps to extract the white matter "skeletons" by taking only the voxels with values higher than 0.2, and then binarize them. These skeletons are considered to represent the white matter (WM), thus we will refer to these as WM masks. We also kept a non-binarized version of the thresholded FA. The second step consists of spatial smoothing of both the thresholded FA maps and to the WM masks with a Gaussian smoothing kernel of $2 \times 2 \times 2$ mm. Finally, we divided the smoothed thresholded FA maps by the smoothed white matter masks. This method was proposed by Lee et al. to compensate for the spatial smoothing effects by dividing the smoothed FA maps and the smoothed tissue specific masks.

Statistical analyses

We compared the FA, AD, RD and MD maps of the subjects from each of the three disease groups to the controls from the same imaging site. A linear regression model was used to adjust for any confounding effects of age in the different diagnostic groups ($p < 0.05$ significance level). In this regression analysis the corresponding FA, AD, RD and MD maps for each child were considered as the outcome variable, while diagnostic group, age and total brain volume were used as predictors. To correct for the increased risk of Type I (false positive) errors due to the thousands of voxel-wise association tests, we used the false discovery rate (FDR) method (Benjamini and Hochberg, 1995) to correct for multiple comparisons. All maps are shown thresholded at the appropriate FDR

critical p-value, where such a threshold exists, to show only regions of significance with an expected 5% false positive rate ($q = 0.05$). Importantly, reported higher critical p-values correspond to greater overall effect on the brain, not an effect size at a particular location. The “critical” p-values used in FDR analysis are not identical to the usual meaning for p-values, which estimate the probability that any given effect has arisen by chance. Instead, the critical p-values show the highest threshold that can be applied to the maps, if there is one, while still being able to say that only 5% of the voxels shown are expected to be false positives. There is no notion of effect size directly corresponding to this p-value, although there is an effect size at each location in the brain. Essentially the critical p-value comes from a cumulative distribution function (histogram) of all the p-values in the map, such that a large number of weak effects or a smaller number of large effects would be counted as significant. As such an impression of the effect size in the map could be inferred from the p-value CDF plot, as we have done in some of our prior papers (Chou et al., 2008).

Quantitative assessment of overlap

We used the Dice coefficient to measure the overlap of the significant areas in the p-maps obtained after the statistical analysis. In doing so, we have to bear in mind that the extent of the significant region depends on the sample size, and with an expanded sample group differences may be detected in more regions. As a result, any statements regarding overlap may be conservative estimates of the regions implicated across multiple disorders. We compared each p-map with significant voxels in it to each of the other p-maps. The results of this analysis are detailed in the Results and Discussion sections below. To ensure a fair comparison between the maps calculated in the both MDTs (MDT-1 and MDT-2), we non-linearly registered MDT-2 to MDT-1. We then applied this transformation to each of the maps in the MDT-2 space with a nearest neighbor interpolation.

Given two sets, the Dice coefficient measures the agreement between them. If A and B are the two sets, the Dice coefficient is given by:

$$D(A, B) = \frac{2|A \cap B|}{|A| + |B|}$$

A value of 0 indicates no overlap; a value of 1 indicates perfect agreement.

Tractography and anatomical location of the areas of significance

We performed whole-brain tractography with a global probabilistic approach based on the voting procedure provided by the Hough transform (Aganj et al., 2011). This algorithm tests candidate 3D curves in the volume, assigning a score to each of them. It then returns the curves with the highest scores as the potential anatomical connections. The score is accordingly derived from the DWI data (for details, please see Aganj et al., 2011). We calculated a total of 10,000 fibers for each subject.

The significant areas within the maps derived from the statistical analysis were transformed back to the each subject’s space, where the tractography was calculated. By doing this, we were able to overlay the significant areas in the space of the subject’s tractography and were able to set them as ROIs to extract and identify the tracts crossing those ROIs.

Results

Girls with 22q11.2 had abnormally lower FA values, relative to corresponding typically developing controls (TD1), in the following regions bilaterally: superior temporal gyri and in the superior corona radiata ($p < 0.00026$), (Fig. 1). This pattern of significance was replicated in the AD maps, where 22q11.2 girls had lower AD and MD in the same regions mentioned above in addition to the middle temporal

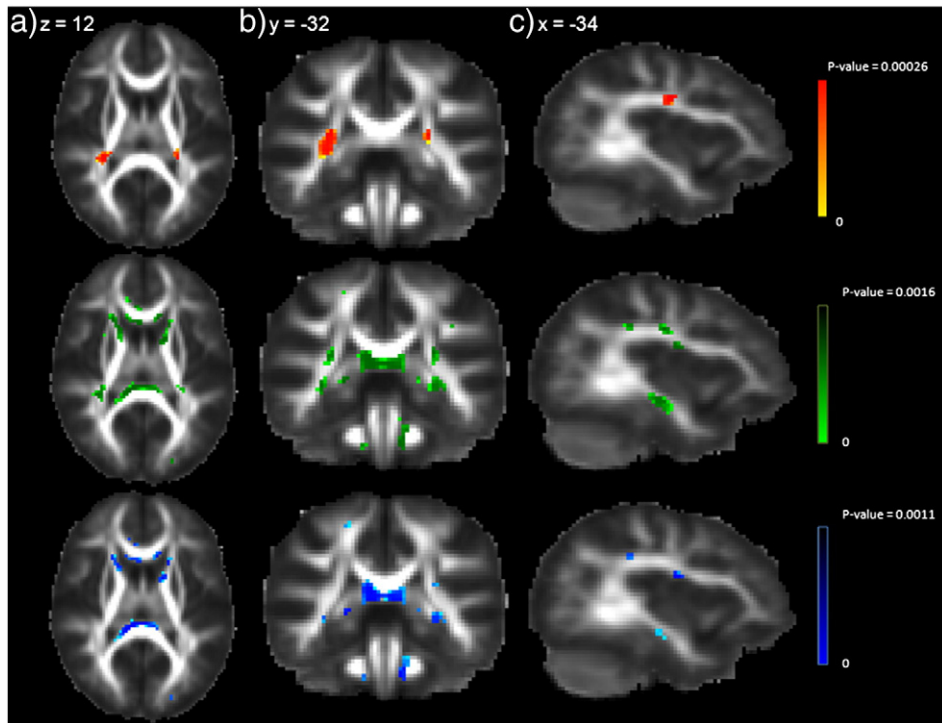


Fig. 1. Superior row: Hot colors depicted in the color bar represent the significant areas with higher FA in typically developing girls than in girls with 22q11.2 (TD > 22q11.2DS). Middle row: Green colors depicted in the color bar represent the significant areas with higher RD in girls with 22q11.2 (22q11.2DS > TD) than in typically developing girls. Bottom row: Blue colors depicted in the color bar represent the significant areas with higher MD in girls with 22q11.2 (22q11.2DS > TD) than in typically developing girls. 0.00026, 0.0016 and 0.0011 represent the critical p-values for each map as determined by the false discovery rate procedure (Benjamini and Hochberg, 1995).

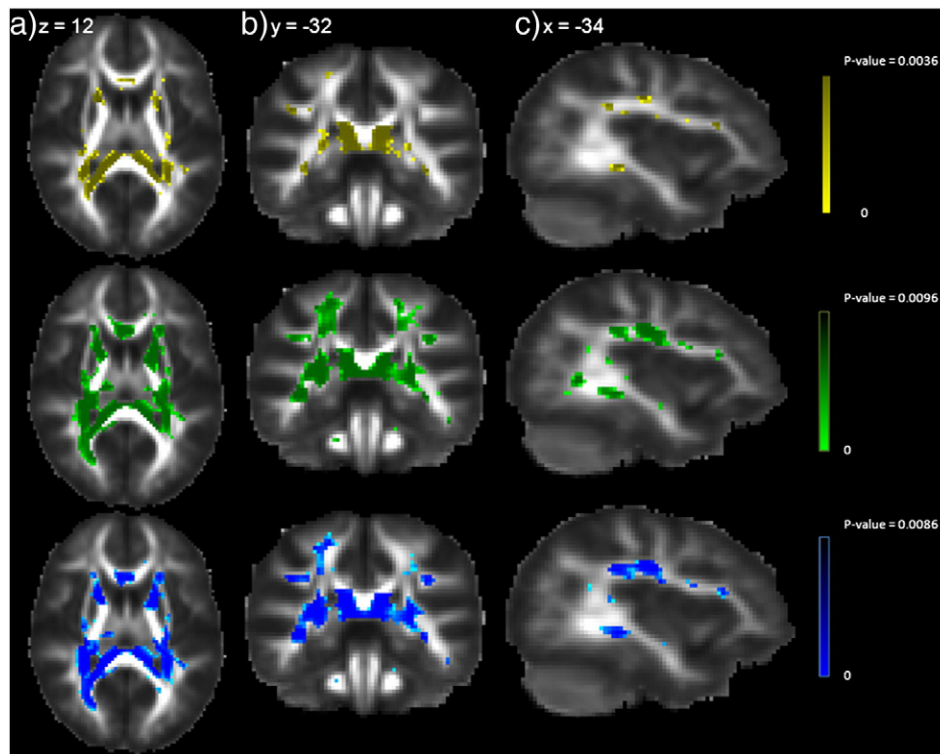


Fig. 2. Superior row: Yellow colors depicted in the color bar represent the significant areas with higher AD in girls with Fragile-X syndrome (FXS > TD) than in typically developing children. Middle row: Green colors depicted in the color bar represent the significant areas with higher RD in girls with Fragile-X syndrome (FXS > TD) than in typically developing girls. Bottom row: Blue colors depicted in the color bar represent the significant areas with higher MD in girls with Fragile-X syndrome (FXS > TD) than in typically developing girls. 0.0036, 0.0096, 0.0086 represent the critical p-values for each map as determined by the false discovery rate procedure (Benjamini and Hochberg, 1995).

gyri and in the right posterior internal capsule ($p < 0.0010$ and $p < 0.0011$, respectively) (Fig. 1).

By contrast, girls with 22q11.2DS had *higher* AD, RD and MD values in regions including clusters in the corpus callosum (genu and splenium), the anterior limb of the internal capsules, external capsules, inferior and posterior parts of the thalami ($p < 0.0010$, 0.0016 and $p < 0.0011$) (Fig. 1). In addition to this, RD and MD maps also showed *higher* diffusivity values in 22q11.2DS where TD1 children have higher FA and AD values as described above (superior *corona radiata* and superior and inferior temporal lobes).

Relative to the TD1 group, girls with FXS showed very similar AD, RD and MD areas of significance ($p < 0.0036$, $p < 0.0096$ and $p < 0.0086$ respectively). These maps showed *higher* diffusivity values, areas including the corpus callosum (splenium and genu), the superior and posterior *corona radiata*, anterior limb of the internal capsules, the external capsules, extended areas of the temporal lobes, occipital lobes, inferior portions of the thalami and central portions of the right thalamus (Fig. 2). No p-values survived the FDR correction when analyzing the FA maps of FXS vs. TD1 girls.

Relative to TD2 controls, girls with TS had *lower* FA in clusters in the superior *corona radiata*, left superior frontal gyrus, corpus callosum (splenium and genu), the anterior and posterior limbs of the internal capsules, cerebral peduncles, and the occipital and temporal lobes ($p < 0.0046$) (Fig. 3). 22q11.2 girls showed significant *higher* diffusivity values in RD and MD maps in the same areas mentioned above, but with less involvement of the internal capsules and the cerebral peduncles ($p < 0.0025$ $p < 0.00068$) (Fig. 3). AD maps of TS vs. TD2 girls were not significantly different.

When analyzing the dice coefficients (DC) resulting from comparing the maps (see Table 3) with statistically significant differences, we found the highest score when comparing the maps where FXS girls had higher AD and RD values than the TD1 controls (DC: 0.8569) (Fig. 2), and when comparing the maps where AD, RD and MD were higher in 22q11.2DS than in TD1 (also see Table 3), where all DC were above 0.6

(better agreement the closer to 1). All of the other comparisons made were below 0.2, where it is worth mentioning the across-syndrome similarities in maps. We found a certain level of overlap between the areas of higher FA in TD2 over TS and the areas of higher AD in FXS than in TD1 (DC: 0.1524). Additionally, the areas where TS had higher RD than TD2 controls overlapped with areas where AD was higher in FXS than in TD1.

There were interesting findings when using the significant clusters from the maps as ROIs to parcellate the tractography results. We used tractographies from the typically developing groups (TD1 and TD2) to better identify the tracts involved. For clarity, we also distinguished the three major types of fibers: long association fibers, projection fibers and commissural fibers (corpus callosum).

Long association fibers

We found the superior longitudinal fasciculus (SLF) to be involved in all three syndromes studied here, as the significant areas in parietal and temporal lobes where FA was lower in 22q11.2DS and TS compared to TD intersected it (Figs. 4, 7). The SLF also passed through areas where the AD, RD, and MD were higher in FXS (Fig. 6) and where RD was higher in 22q11.2DS (Fig. 8).

The inferior longitudinal fasciculus (ILF) also intersected areas in the temporal and occipital lobes where FA was lower in 22q11.2DS and TS (Figs. 4 and 7), especially in the right hemisphere. The ILF could also be identified crossing regions where the AD, RD and MD were higher in 22q11.2DS and FXS (Figs. 6 and 8), as well as where RD and MD were higher in TS. In all these maps, tractography showed that the ILF was more clearly involved on the right hemisphere.

The inferior fronto-occipital fasciculus (IFO) was found to be intersecting significant clusters in the right hemisphere where FA was lower in TS (Fig. 4) and where AD, RD and MD were higher in FXS girls (Fig. 6). Also some IFO fibers were identified intersecting small clusters with lower RD and MD in TS girls (Fig. 4). The intersecting

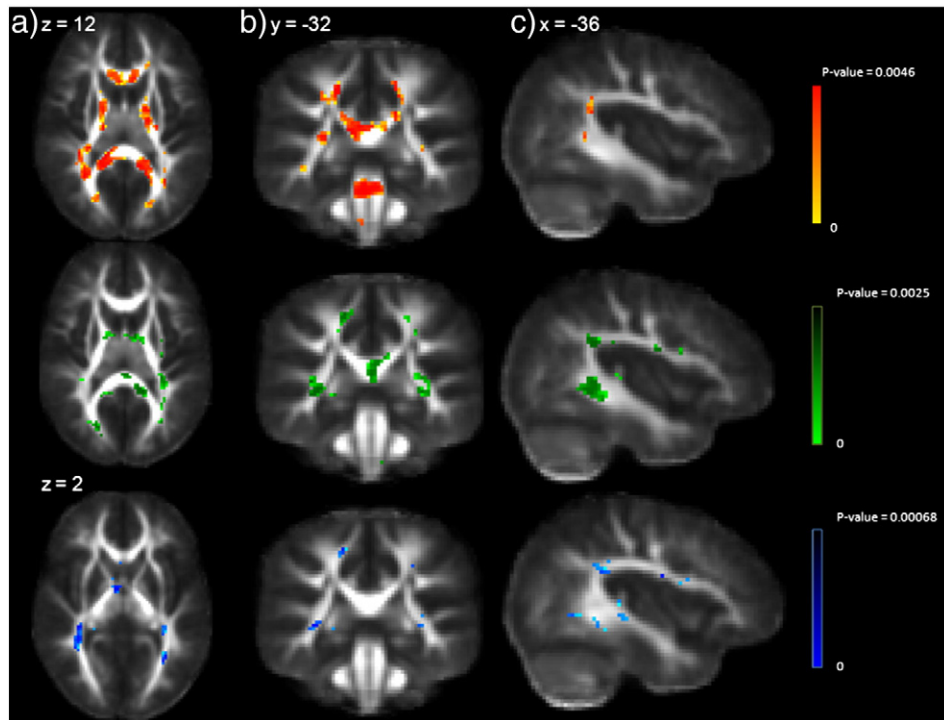


Fig. 3. Superior row: Hot colors depicted in the color bar represent the significant areas with higher AD in girls with Turner syndrome (TS > TD) than in typically developing children. Middle row: Green colors depicted in the color bar represent the significant areas with higher RD in girls with Turner syndrome (TS > TD) than in typically developing girls. Bottom row: Blue colors depicted in the color bar represent the significant areas with higher MD in girls with Turner (TS > TD) than in typically developing girls 0.0046, 0.0025 and 0.00068 represent the critical p-values in each map as determined by the false discovery rate procedure (Benjamini and Hochberg, 1995).

clusters were mainly seen in the temporal and occipital lobes and in the anterior limbs of the external capsules.

Projection fibers and corpus callosum

In general, the significant scattered clusters that were found within the central and posterior *corona radiata* were intersected by a myriad of projection fibers (cortico-thalamic, cortico-spinal, cortico-cerebellar). We noticed a pattern where FXS girls had higher AD, RD, and MD than TD1 controls (Fig. 6), where TS had lower FA and higher MD and RD than TD2 (Fig. 5) and where 22q11.2DS girls had higher AD and RD than TD1 (Fig. 7). These areas were also intersected by some fibers from the body of the corpus callosum.

We could also see cortico-thalamic projection fibers running through statistically significant clusters of the postero-inferior sections of the thalami to the occipital lobe. This pattern was seen where FXS had

higher AD, RD, and MD than TD1 and in areas where 22q11.2DS had higher AD and RD than TD2 controls.

As mentioned above, the anterior limb of the internal capsule had higher AD, RD and MD in FXS and lower FA and higher RD and MD in TS. This area was crossed by projection fibers to the frontal lobe (Figs. 4, 6 and 8).

Discussion

The current study aimed to test the hypothesis that, given the phenotypic overlap in three different genetic syndromes (22q11.2DS, FXS, TS), there would be broad white matter structural differences and similarities determined across these groups compared to typically developing children in regions known to be related to visuospatial and numerical processing.

We found patterns of statistical differences of typical developing children having significantly higher FA values than atypically developing ones, which were also replicated in the diffusivity maps where non-typical developing children had higher diffusivity values than controls. This pattern of findings was evident when measuring the overlap of these maps (Table 3). FA is said to account for white matter fiber integrity and fascicle coherence. In general, we expect higher diffusivities in areas where FA is diminished (Thomason and Thompson, 2011). In one case, our results for FXS compared to TD did not show significant differences for FA but rather widespread differences in all three diffusivity measures within the white matter.

Clearly, differences in FA and diffusivity measures between typical and non-typical children do not necessarily have the same causes in each of the three disorders studied here. Even so, pathological evidence supports some similarities among the three conditions. In general, FA, AD, RD and MD depend mainly on structural variables such as axonal packing, myelination, membrane permeability to water, internal axonal structure, and intra-axonal space (Assaf et al., 2008). For example pathological findings in TS point out the prevalence of cortical organization

Table 3

In this table we show the highest scores after calculating the dice coefficient when comparing the maps where FA, AD, RD, and MD were significantly higher in 22q11.2 deletion syndrome (22Q), Fragile X syndrome (FXS), and Turner syndrome (TS) over their corresponding typical developing group (TD1 and TD2) or vice versa. In bold: The comparisons across syndromes that resulted with a relatively higher score.

MAPS COMPARISON	Dice coefficient
RD/FXS_over_TD1 vs. MD/FX_over_TD1	0.856
AD/22Q_over_TD1 vs. MD/22Q_over_TD1	0.836
RD/22Q_over_TD1 vs. MD/22Q_over_TD1	0.781
AD/22Q_over_TD1 vs. RD/22Q_over_TD1	0.640
AD/TD1_over_22Q vs. MD/TD1_over_22Q	0.170
FA/TD2_over_TS vs. AD/FX_over_TD1	0.152
FA/TD1_over_22Q vs. AD/TD1_over_22Q	0.121
FA/TS_over_TD2 vs. MD/TS_over_TD2	0.118
AD/FX_over_TD1 vs. RD/TS_over_TD2	0.102
RD/TD1_over_22Q vs. MD/TD1_over_22Q	0.083

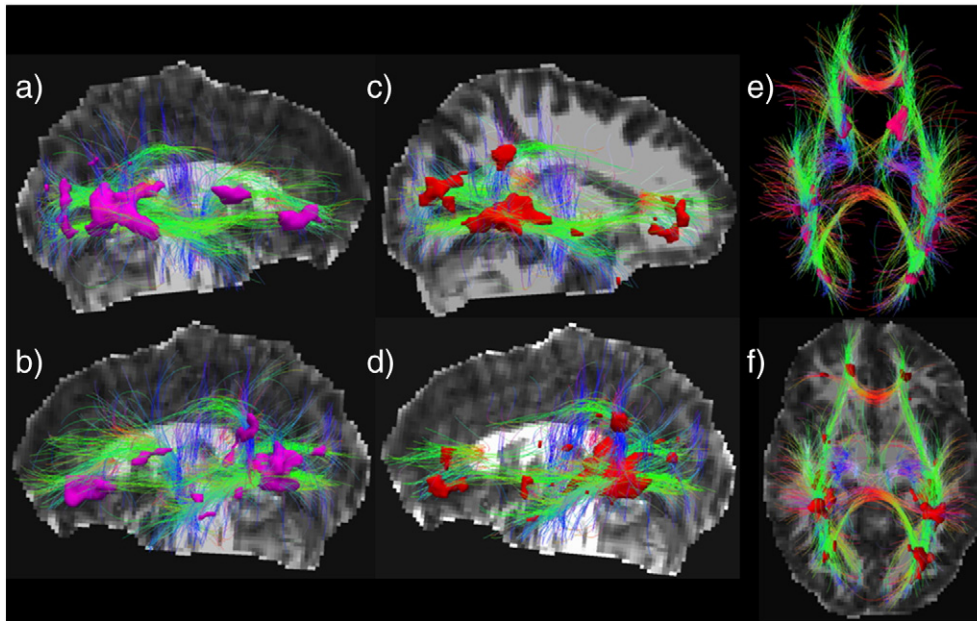


Fig. 4. a), b) and e) Tractography shows fibers from long association fasciculi (SLF, ILF and IFO) after being seeded with clusters of lower FA in Turner syndrome. c), d) and f) Tractography after being seeded with clusters of higher RD in Turner syndrome. Subject: 13.16 year old typically developing girl.

abnormalities such as cortical dysplasia, pachygyria and polymicrogyria, and posterior fossa malformations that may ultimately alter axonal packing in the white matter (Della Giustina et al., 1985; Terao et al., 1996; Tombini et al., 2003). Myelin has been reported as normal in TS though (Palo and Savolainen, 1973; Sy et al., 2010). In 22q11.2DS, there have been radiological and pathological reports of cortical dysgenesis and abnormal gyrification patterns in some patients (Kiehl et al., 2009; Robin et al., 2006; Schaer et al., 2006; Sztriha et al., 2004). There is also experimental evidence of abnormal neuronal proliferation and migration in early stages of development resulting in an altered cortical connectivity pattern (Meechan et al., 2009). Focal myelin damage in 22q11.2DS has been related to post-developmental vascular events and microvascular anomalies caused by dysregulated angiogenesis. Experimental evidence in FXS has revealed abnormal dendritic spine lengths and shapes on

neocortical pyramidal cells, but no other major neuropathological abnormalities have been reported (Irwin et al., 2000; Rudelli et al., 1985; Wisniewski et al., 1991). These findings suggest the failure of normal dendritic spine maturation, and/or pruning, but not neurogenesis or migration problems. Thus, in the three diseases, the neuropathogenesis is more related to disrupted connectivity in early or later phases of development. Abnormal neuronal connectivity, either locally or throughout the entire brain, may ultimately affect axonal integrity and adequate packing of axonal bundles. This may lead to atypical developmental trajectories as has been demonstrated for 22q11.2DS, for example (Simon et al., 2008b).

Our findings show lower FA and AD plus higher MD and RD values in 22q11.2DS children especially in posterior regions of the brain (parietal, occipital and posterior temporal lobes), mainly in areas intersecting the inferior longitudinal fasciculus (ILF), superior longitudinal fasciculus

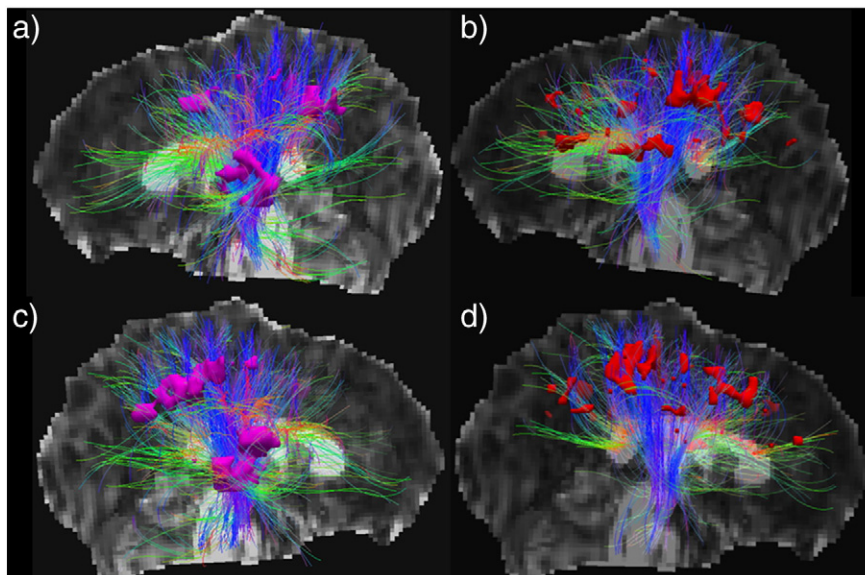


Fig. 5. The four figures show extensive projection fibers (corticospinal and corticothalamic). Seeds on the left side represent areas of lower FA in Turner syndrome and on the right side higher RD in Turner syndrome. Subject: 13.16 year old typically developing girl.

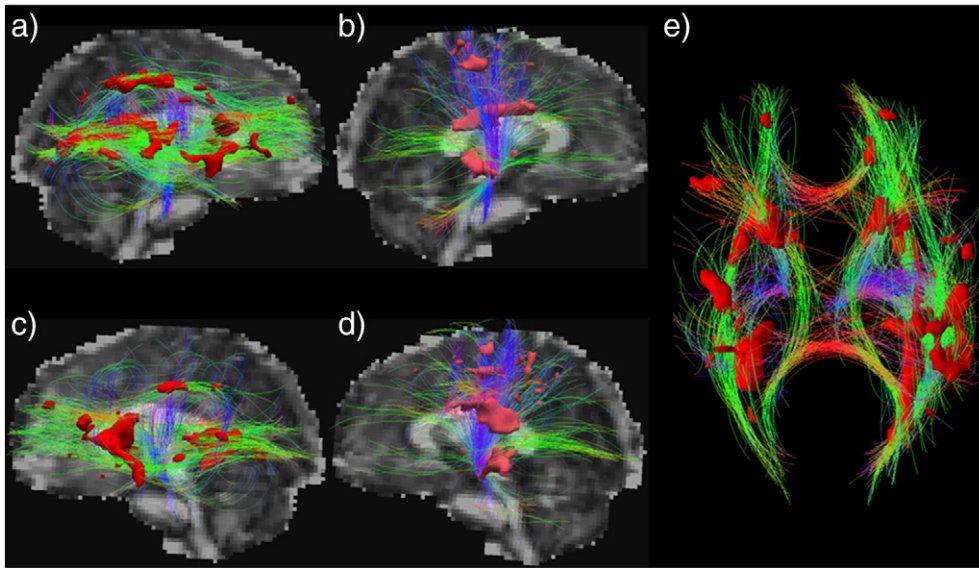


Fig. 6. a) c) and e) show dissected long association fibers (SLF, ILF and IFO) after seeding the tractography with areas of high RD and MD in Fragile-X girls. b) and d) show the same tractography but the projection fibers are dissected here. Notice the optic radiation fibers in posterior section of the brain. Subject: 13 years old typically developing girl.

(SLF) (Figs. 1, 7 and 8). Prior studies also reported lower anisotropy in areas corresponding to the SLF (Barnea-Goraly et al., 2003b; Simon et al., 2008b). Simon et al. (2008b) also found significant lower anisotropy in the external capsules, which they considered to be part of the inferior longitudinal fasciculus (IFO) and in a similar fashion our analysis also revealed increased RD and MD in the same location. Other regions of interest in participants with 22q11.2DS included significantly lower FA values and higher AD, RD and MD in bilateral clusters in the inferior and posterior part of the thalami which we could demonstrate that is where a bundle of fibers projecting to the occipital cortex is originating. When analyzing FA values in the parietal white matter, Barnea-Goraly et al. found a positive correlation between FA and arithmetic scores achieved by subjects with 22q11.2DS in the left parietal lobe. In addition to this, in a study using DTI data acquired at 1.5 T, with 6 diffusion gradient directions and a coarser in-plane matrix, Simon et al. reported differences in the parietal lobes of 22q11.2DS children (girls and boys together) consisting of significant direct correlation of higher FA and higher AD to poorer performance on a visuospatial attention task that would be expected to involve contiguous cortex. According to the authors, this suggests a lower degree of connectivity of the parietal cortex to surrounding cortex (Simon et al., 2005b, Simon et al., 2008b). Although we were not able to correlate our neuroimaging measures with visuospatial and arithmetic performance, we did find higher AD (as well as RD) but not FA in the parietal white matter of 22q11.2DS girls. This may be due to differences in the acquisition parameters for the DTI data, although its cause is not entirely clear.

Our findings of 22q11.2DS white matter abnormalities are related to previous volumetric morphometry studies. Besides having lower brain volumes (by 8–11%) (Eliez et al., 2000; Kates et al., 2001; Simon et al., 2005b), in both gray and white matter, reductions are more localized towards the cerebellum and parietal, temporal and occipital lobes, which are in the posterior regions of the brain. ROI-based studies of structural MRI found reduced white matter volumes in areas in the parietal, occipital and temporal regions (van Amelsvoort et al., 2001). Reduced gray and white matter in superior temporal regions has also been associated with the increase psychosis risk in this population (Chow et al., 2011; Gothelf et al., 2007a,b). Decreased volumes of posterior thalamic nuclei in children with 22q11.2DS (Bish et al., 2004) have been reported as well.

We found areas of significant differences of FA and diffusivity measures at the edges of the corpus callosum in children with 22q11.2DS,

more specifically at the genu and the splenium (Fig. 1). There is considerable evidence showing volumetric differences of the corpus callosum, the lateral ventricles and thalami between typical developing children and 22q11.2DS children. Prior volumetric studies of the corpus callosum found a generally increased volume in individuals with 22q11.2DS, particularly in the isthmus (Shashi et al., 2004) and rostrum (Machado et al., 2007) but also in the splenium (van Amelsvoort et al., 2001). Machado et al. also found a significant correlation between ventricular enlargement and corpus callosum curvature along the rostral body, posterior midbody, isthmus and splenium of the 22q11.2DS individuals (Machado et al., 2007). In addition to this, Simon et al. reported higher FA values within the splenium in typically developing children (Barnea-Goraly et al., 2003b; Simon et al., 2005b), which is consistent with our findings, and they concluded after a voxel-based morphometry analysis comparing TD and 22q11.2DS that these findings in the corpus callosum were explained by a change in location and morphology of this structure due to enlarged lateral ventricles in the 22q11.2DS population. Additionally, there is evidence of decreased volume in the thalamus – particularly in its posterior nuclei (Bish et al., 2004), which may also add to the structural differences surrounding the lateral ventricles. Further analysis of this area is required to identify areas of the splenium with significant FA differences that are not merely due to volumetric differences between populations.

Prior fMRI studies have suggested disrupted fronto-parietal connectivity in subjects with 22q11.2DS. Children with 22q11.2DS have shown functional abnormalities within this network, for example abnormally increased activations in prefrontal, precentral gyrus and parietal cortex when solving arithmetical tasks. Additionally, there was increased activity in supramarginal gyrus when solving numerical computation tasks of greater difficulty (Eliez et al., 2001b) as opposed to a steady normal frontal and parietal activation in control subjects. The authors argued this to be related to the need to recruit more resources to perform the tasks. In another study, 22q11.2DS children and adolescents were compared to TD controls during a spatial working memory task (Azuma et al., 2009), researchers found a greater activation in the TD group than in children with 22q11.2DS in the parietal and occipital regions with no significant difference in activation of frontal regions (dorsolateral prefrontal cortex).

Although we did not find significant differences in FA between FXS girls and controls, our study did find an increase in all three diffusivity measures (AD, RD and MD) in FXS girls in a very similar fashion (Fig. 2

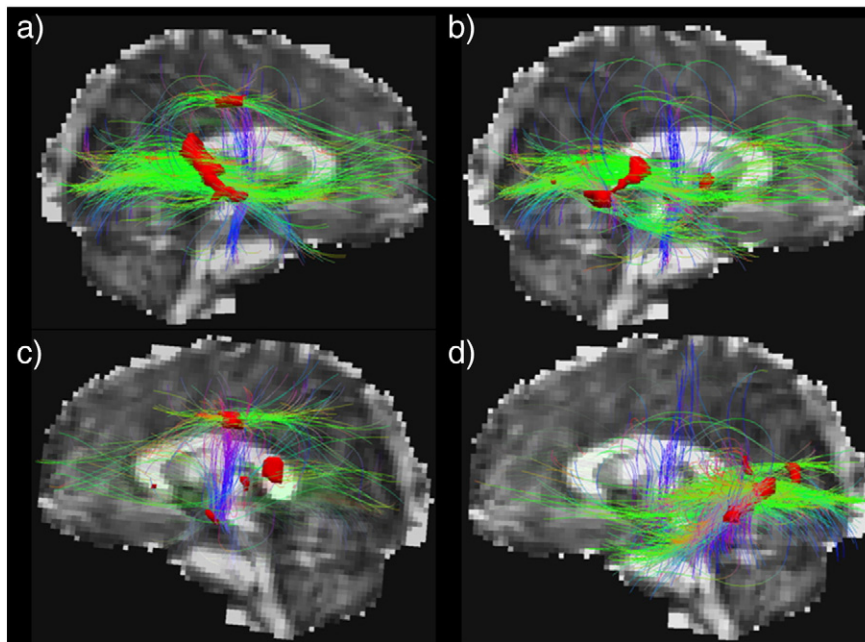


Fig. 7. a) and c) show right ILF and SLF and left SLF in a typically developing girl of 13 years old. Seeds correspond to regions of lower FA in 22q11.2DS. b) and d) show same subject's tractography seeded with clusters of lower AD in 22q11.2DS ($TD > 22q11.2DS$). Notice the ILF in both hemispheres.

and Table 3). These significant clusters were consistent with previous DTI findings of lower FA in the *corona radiata* and *centrum semiovale* (Barnea-Goraly et al., 2003a) and our findings do also extend to the temporal and occipital lobes, internal and external capsules, corpus callosum and thalami. These areas involve SLF, ILF, and IFO fibers. Previous volumetric studies have found increased white matter in temporal and parietal lobes of FXS children (Lee et al., 2007), areas where these tracts travel through. Also some fMRI studies that have investigated arithmetic abilities and working memory function in FXS children have pointed out a dysfunction in the fronto-parietal networks. Rivera et al. (2002) investigated arithmetic processing in females with FXS versus typically developing controls (Rivera et al., 2002) and they found impaired activation of the superior frontal gyrus during arithmetic tasks in part of a network including the parietal lobe. That study showed that individuals with FXS were

unable to modulate activation in prefrontal and parietal cortex, as evidenced by an inability to recruit new neural resources in response to increasing cognitive load. Studies evaluating attention in subjects with FXS revealed a network between the thalamus, the basal ganglia, the cingulate, the temporal and occipital cortex and the ventrolateral and dorsolateral prefrontal cortex (VLPFC and DLPFC, respectively). This network is heavily modulated by the FMRP levels and, in general, FXS shows impaired activation of the VLPFC and DLPFC compared to typical developing controls (Menon et al., 2004; Hoefft et al., 2007b).

To the best of our knowledge, there are no reports on corpus callosum structural or functional abnormalities in FXS. Our prior tensor-based morphometry study (Lee et al., 2007), in a non-overlapping cohort, compared age-matched FXS subjects (mean age 14 years) with normal controls. There, we found increased volume in periventricular white matter,

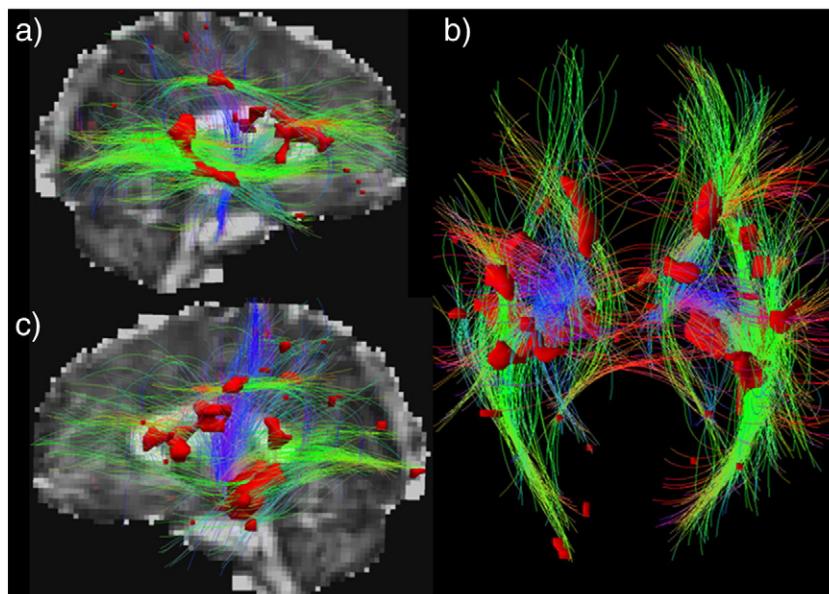


Fig. 8. a) b) and c) show a tractography of a 13 year old typical developing girl seeded with areas of higher RD and MD in 22q11.2DS girls. Notice the SLF and ILF in both hemispheres and the IFO in the right hemisphere.

parietal and temporal subcortical white matter, as well as enlarged lateral ventricles. It is unknown how much of this white matter volume increase is due to alteration in the corpus callosum fiber structure. There is a paucity of DTI studies of FXS, so our findings in the corpus callosum need further validation and replication.

TS is a heterogeneous disorder that includes women with different genotypes such as complete monosomy X (45,X karyotype), isochromosomes (46,X,i[Xq]), rings (46,X,r[X]), deletions (46,X,del[Xp] or 46,X,del[Xq]), and mosaicism (Held et al., 1992). Additionally, many women with TS receive estrogen replacement therapy due to ovarian failure, which adds another variable that may influence the brain's developmental trajectory. Three studies have investigated white matter structure with DTI in TS. Each of these studies has examined different populations with TS in terms of their genotype and onset of hormonal replacement therapy at the time of data acquisition. The first study using DTI in TS included a mixture of mosaic and nonmosaic TS young adult women, and all but one of whom were being treated with estrogens (Molko et al., 2004). They found higher FA values in TS women in both superior temporal sulci and the right centrum semiovale and right external capsule, and no there were significant regions with lower FA. Nonetheless, MD was higher in TS women in the right fusiform gyrus and in the occipitotemporal region, bilaterally. Subsequently, Holzapfel et al. (2006) examined a sample of only nonmosaic children and young adults—all but two were receiving hormonal treatment. Their results showed lower FA in TS in the deep left frontoparietal white matter (SLF), in the right prefrontal cortex close to the caudate, and in the internal capsules, bilaterally. These locations were also significant in the same study for reduced white matter density, as seen with VBM, and TBM. Additionally, the TS group exhibited higher FA values in the right precentral gyrus and in the temporal gyri.

The latest of these studies (Yagamata et al., 2011) investigated the white matter of a very similar cohort to ours, namely only 45, X karyotype, nonmosaic girls, none of them with estrogen treatment. Using TBSS (Smith et al., 2006) and an atlasbased approach they found lower FA in these girls in regions of the white matter very similar to ours: the SLF bilaterally (more prominent on the left side), the ILF (more prominent on the left) and the IFO, although we found the right ILF to have more areas with significant differences. They also found lower FA in extended areas of the corpus callosum, including the splenium, body, genu and tapetum, as well as in the corticospinal tract, anterior and posterior thalamic radiations. We consistently found lower FA in TS in these areas as well. They report finding areas of lower FA in the left external capsule, where we did not find any significant difference between TS and control girls.

Our study has the limitation of not having the cognitive tests available of the TS girls, which makes the results more difficult to interpret in terms of their relevance for cognition and behavior, and also implies that we cannot make strong generalizations to other cohorts who may differ cognitively or behaviorally. Even so, our cohort of TS girls is genetically homogeneous as well as clinically in terms of the estrogen replacement therapy and many of our findings were highly consistent with findings reported in prior studies. Some white matter regions have been consistently found to be altered in all the studies – in particular, the occipitotemporal region, which contains fibers of the ILF and IFO. The SLF, especially on the left side, and the internal capsules bilaterally – which are crossed by a myriad of projection fibers have been reported to be altered in two of the studies mentioned above that analyzed only nonmosaic girls, as well as in ours. This suggests that there may be white matter structural abnormalities in TS that are not affected by hormonal replacement therapy and that depend more on the specific genetic load given by the sex chromosomes in earlier stages of brain development. SLF, ILF and IFO are association tracts that connect the frontal lobe to the more posterior regions of the parietal, occipital and temporal lobes. They are thought to play an important role in the transport of information between these

areas, particularly in visuospatial tasks, attention and numerical reasoning. Behavioral studies support the view that visuospatial and perceptual deficits in TS (mosaic and nonmosaic) persist from childhood into adulthood and do not improve with estrogen replacement, whereas motor and certain memory functions respond to this kind of therapy (Ross et al. 2000; Ross et al., 2002). In addition to this, fMRI studies on nonmosaic and mosaic adult women with TS have shown impaired frontoparietal activation during numerical tasks and visuospatial paradigms while being on estrogen therapy (Molko et al., 2003; Hart et al. 2006). In the future, efforts should be directed towards imaging studies with more homogeneous populations with TS, while taking into account important cognitive and therapeutic aspects in these women.

We did find common abnormalities shared by the 3 syndromes. The most prominent commonality was the finding of altered FA and diffusivity of the SLF in the three syndromes. In 22q11.2DS this region showed lower FA and higher AD, RD and MD, most prominently on the left side (Figs. 7 and 8). The SLF showed higher AD, RD and MD in FXS (Fig. 6) and in TS the same region showed higher RD and MD and lower FA in both hemispheres (Fig. 4). Prior DTI studies on the anatomy of the SLF have been able to correlate the anatomy of this fasciculus with its counterpart in non-human primates. It has been divided into three sections: a fronto-parietal component that runs lateral to the projection fibers of the corona radiata (SLF I), a temporo-parietal part that runs around the Sylvian fissure (SLF II) and a more lateral one that penetrates the perisylvian cortex (SLF III) (Catani and Thiebaut de Schotten, 2008). Interestingly, we found that the altered section in TS is the temporo-parietal section (SLF II), whereas for 22q11.2DS and for FXS the fronto-parietal section is clearly involved (SLF I). The SLF is part of brain networks processing language, spatial working memory and numerical tasks on the left side (van Eimeren et al., 2010; Vestergaard et al., 2010), to visuospatial attention in the right side (de Schotten et al., 2011). Interestingly, numerical ability tends to show positive correlations with FA values in the left SLF (van Eimeren et al., 2010). As we noted before, for all three syndromes there is substantial evidence that fronto-parietal connectivity is disrupted, and this may contribute to poorer performance on tasks involving attention, visuospatial working memory and arithmetic. Despite the age range of our cohort, and that the SLF anisotropy and diffusivity signals are not fully mature until the mid-teen years (Lebel et al., 2008, Qiu et al., 2008), we were still able to see differences. In terms of known functions of the SLF, we could not find an explanation to account for different sections of this tract being involved TS vs. FXS/22q11.2DS.

We found the ILF to be altered in the three syndromes, but whereas the differences could be seen bilaterally in the TS and FXS subjects (lower FA and higher diffusivity values), the findings were unilateral in 22q11.2DS children. FA was clearly lower and MD and RD higher in the right ILF in these subjects and TD controls had higher AD values bilaterally. Very similar effects were also found for the IFO, which intersected significant clusters in the external capsules and frontal lobes in TS and FXS, but not in 22q11.2DS where its fibers showed differences mainly on the right side. The ILF connects the occipital and temporal lobes and is involved in visual perception (Ffytche, 2008) and face processing (Fox et al., 2008). Different functional studies have found impairments in the occipito-temporal network in facial recognition and verbal processing in FXS and 22q11.2DS (van Amelsvoort et al., 2006; Holsen et al., 2008). The role of the IFO in these syndromes' cognition and executive functions is less clear, but there is some evidence linking this tract to visual processing and attention (Fox et al., 2008; Doricchi et al., 2008).

The role of the different projection fibers connecting the thalamus and basal ganglia to the frontal lobes through the internal capsules and the optic radiations towards the occipital lobe is less clear for visuospatial attention and executive functions, as well as numerical abilities. Further evidence of the role of these fibers in visuospatial attention and executive function is still to be found.

In summary, we investigated the white matter integrity profile across females with three defined genetic disorders. Many regions with significant differences across the three diseases do not completely overlap, but many of the same major tracts are implicated. Common abnormalities were evident in 22q11.2DS and TS, where SLF and ILF had lower anisotropy and diffusivity and FXS had higher diffusivities. Additionally we found thalamic-frontal and thalamic-occipital fibers to be altered in 22q11.2DS, FXS, and TS.

Conflict of interest

None.

Acknowledgments

This work was supported by grants NIH HD46159 and NIH HD42974 (to T.J.S.). Additional support was provided by R01 grants EB008432, EB008281, and EB007813 (to P.T.) and by the National Library of Medicine (T15 LM07356; to N.J.). The funding source had no role in the study design, collection, analysis and interpretation of data, writing of the report, or in the decision to submit the article for publication.

References

- Aganj, I., Lenglet, C., Jahanshad, N., Yacoub, E., Harel, N., Thompson, P.M., Sapiro, G., 2011. A Hough transform global probabilistic approach to multiple-subject diffusion MRI tractography. *Med. Image Anal.* 15, 414–425.
- Arnold, A.P., Gorski, R.A., 1984. Gonadal steroid induction of structural sex differences in the central nervous system. *Annu. Rev. Neurosci.* 7, 413–442.
- Assaf, Y., Blumenfeld-Katzir, T., Yovel, Y., Basser, P.J., 2008. Axcaliber: a method for measuring axon diameter distribution from diffusion MRI. *Magn. Reson. Med.* 59, 1347–1354.
- Azuma, R., Daly, E., Campbell, L., Stevens, A., Deeley, Q., Giampietro, V., Brammer, M., Glaser, B., Ambery, F., Morris, R., Williams, S., Owen, M., Murphy, D., Murphy, K., 2009. Visuospatial working memory in children and adolescents with 22q11.2 deletion syndrome: an fMRI study. *J. Neurodev. Disord.* 1, 46–60.
- Barnea-Goraly, N., Eliez, S., Hedeus, M., Menon, V., White, C.D., Moseley, M., Reiss, A.L., 2003a. White matter tract alterations in Fragile X syndrome: preliminary evidence from diffusion tensor imaging. *Am. J. Med. Genet. B Neuropsychiatr. Genet.* 118B, 81–88.
- Barnea-Goraly, N., Menon, V., Krasnow, B., Ko, A., Reiss, A., Eliez, S., 2003b. Investigation of white matter structure in velocardiofacial syndrome: a diffusion tensor imaging study. *Am. J. Psychiatry* 160, 1863–1869.
- Beaton, E.A., Qin, Y., Nguyen, V., Stoddard, J., Pinter, J.D., Simon, T.J., 2010. Increased incidence and size of cavum septum pellucidum in children with chromosome 22q11.2 deletion syndrome. *Psychiatry Res. Neuroimaging* 181, 1081–113.
- Bearden, C.E., Woodin, M.F., Wang, P.P., Moss, E., McDonald-McGinn, D., Zackai, E., Emmanuel, B., Cannon, T.D., 2001. The neurocognitive phenotype of the 22q11.2 deletion syndrome: selective deficit in visual-spatial memory. *J. Clin. Exp. Neuropsychol.* 23, 447–464.
- Benjamini, Y., Hochberg, Y., 1995. Controlling the false discovery rate: a practical and powerful approach to multiple testing. *J. R. Stat. Soc. Ser. B Methodol.* 57, 289–300.
- Bish, J.P., Nguyen, V., Ding, L., Ferrante, S., Simon, T.J., 2004. Thalamic reductions in children with chromosome 22q11.2 deletion syndrome. *Neuroreport* 15, 1413–1415.
- Bishop, D.V., Canning, E., Elgar, K., Morris, E., Jacobs, P.A., Skuse, D.H., 2000. Distinctive patterns of memory function in subgroups of females with Turner syndrome: evidence for imprinted loci on the X-chromosome affecting neurodevelopment. *Neuropsychologia* 38, 712–721.
- Bittel, D.C., Yu, S., Newkirk, H., Kibiryaeva, N., Holt, A., Butler, M.G., Cooley, L.D., 2009. Refining the 22q11.2 deletion breakpoints in DiGeorge syndrome by aCGH. *Cytogenet. Genome Res.* 124, 113–120.
- Braddick, O., Atkinson, J., Wattam-Bell, J., 2003. Normal and anomalous development of visual motion processing: motion coherence and 'dorsal-stream vulnerability'. *Neuropsychologia* 41, 1769–1784.
- Brown, W.E., Kesler, S.R., Eliez, S., Warsofsky, I.S., Haberecht, M., Reiss, A.L., 2004. A volumetric study of parietal lobe subregions in Turner syndrome 46 (9), 607–609.
- Brown, W.E., Kesler, S.R., Eliez, S., Warsofsky, I.S., Haberecht, M., Patwardhan, A., Ross, J.L., Neely, J.L., Zeng, S.M., Yankowitz, J., Reiss, A.L., 2002. Brain development in Turner syndrome: a magnetic resonance imaging study. *Psychiatry Res. Neuroimaging* 116 (3), 187–196.
- Bruandeta, M., Molkoa, N., Cohena, L., Dehaene, S., 2004. A cognitive characterization of dyscalculia in Turner syndrome. *Neuropsychol.* 42 (3), 288–298.
- Burn, J., Goodship, J., 1996. Developmental genetics of the heart. *Curr. Opin. Genet. Dev.* 6, 322–325.
- Catani, M., Thiebaut de Schotten, M., 2008. A diffusion tensor imaging tractography atlas for virtual in vivo dissections. *Cortex* 44, 1105–1132.
- Chou, Y.-Y., Lepore, N., de Zubicaray, G.I., Carmichael, O.T., Becker, J.T., Toga, A.W., Thompson, P.M., 2008. Automated ventricular mapping with multi-atlas fluid image alignment reveals genetic effects in Alzheimer's disease. *Neuroimage* 40, 615–630.
- Chow, E.W.C., Ho, A., Wei, C., Voormolen, E.H.J., Crawley, A.P., Bassett, A.S., 2011. Association of schizophrenia in 22q11.2 deletion syndrome and gray matter volumetric deficits in the superior temporal gyrus. *Am. J. Psychiatry* 168, 522.
- Cornish, K.M., Munir, F., Cross, G., 1999. Spatial cognition in males with Fragile-X syndrome: evidence for a neuropsychological phenotype. *Cortex* 35, 263–271.
- Crawford, D.C., Meadows, K.L., Newman, J.L., Taft, L.F., Pettay, D.L., Gold, L.B., Hersey, S.J., Hinkle, E.F., Stanfield, M.L., Holmgren, P., Yeargin-Allsopp, M., Boyle, C., Sherman, S.L., 1999. Prevalence and phenotype consequence of FRAXA and FRAXE alleles in a large, ethnically diverse, special education-needs population. *Am. J. Hum. Genet.* 64, 495–507.
- de Schotten, M.T., Dell'Acqua, F., Forkel, S.J., Simmons, A., Vergani, F., Murphy, D.G.M., Catani, M., 2011. A lateralized brain network for visuospatial attention. *Nat. Neurosci.* 14, 1245–1246.
- De Smedt, B., Devriendt, K., Fryns, J.P., Vogels, A., Gewillig, M., Swillen, A., 2007. Intellectual abilities in a large sample of children with velo-cardio-facial syndrome: an update. *J. Intellect. Disabil. Res.* 51, 666–670.
- Della Giustina, E., Forabosco, A., Botticelli, A., Pace, P., 1985. Neuropathology of the Turner syndrome. *Pediatr. Med. Chir.* 7, 49.
- Doricchi, F., Thiebaut de Schotten, M., Tomaiuolo, F., Bartolomeo, P., 2008. White matter (dis) connections and gray matter (dys) functions in visual neglect: gaining insights into the brain networks of spatial awareness. *Cortex* 44, 983–995.
- Eliez, S., Schmitt, J.E., White, C.D., Reiss, A.L., 2000. Children and adolescents with velocardiofacial syndrome: a volumetric MRI study. *Am. J. Psychiatry* 157, 409–415.
- Eliez, S., Blasey, C.M., Freund, L.S., Hastie, T., Reiss, A.L., 2001a. Brain anatomy, gender and IQ in children and adolescents with Fragile X syndrome. *Brain* 124, 1610–1618.
- Eliez, S., Blasey, C.M., Menon, V., White, C.D., Schmitt, J.E., Reiss, A.L., 2001b. Functional brain imaging study of mathematical reasoning abilities in velocardiofacial syndrome (del22q11.2). *Genet. Med.* 3, 49–55.
- Farzin, F., Rivera, S.M., 2010. Dynamic object representations in infants with and without Fragile X syndrome. *Front. Hum. Neurosci.* 4.
- Farzin, F., Whitney, D., Hagerman, R.J., Rivera, S.M., 2008. Contrast detection in infants with Fragile X syndrome. *Vision Res.* 48, 1471–1478.
- ffytche, D.H., 2008. The hodology of hallucinations. *Cortex* 44, 1067–1083.
- Fonov, V., Evans, A.C., Botteron, K., Almli, C.R., McKinstry, R.C., Collins, D.L., 2011. Unbiased average age-appropriate atlases for pediatric studies. *Neuroimage* 54, 313–327.
- Fox, C.J., Iaria, G., Barton, J.J.S., 2008. Disconnection in prosopagnosia and face processing. *Cortex* 44, 996–1009.
- Freund, L.S., Reiss, A.L., 1991. Cognitive profiles associated with the fra(X) syndrome in males and females. *Am. J. Med. Genet.* 38, 542–547.
- Galvez, R., Greenough, W.T., 2005. Sequence of abnormal dendritic spine development in primary somatosensory cortex of a mouse model of the Fragile X mental retardation syndrome. *Am. J. Med. Genet. A* 135A, 155–160.
- Gothelf, D., Feinstein, C., Thompson, T., Gu, E., Penniman, L., Van Stone, E., Kwon, H., Eliez, S., Reiss, A.L., 2007a. Risk factors for the emergence of psychotic disorders in adolescents with 22q11.2 deletion syndrome. *Am. J. Psychiatry* 164, 663–669.
- Gothelf, D., Penniman, L., Gu, E., Eliez, S., Reiss, A.L., 2007b. Developmental trajectories of brain structure in adolescents with 22q11.2 deletion syndrome: a longitudinal study. *Schizophr. Res.* 96, 72–81.
- Green, T., Gothelf, D., Glaser, B., Debbane, M., Frisch, A., Kotler, M., Weizman, A., Eliez, S., 2009. Psychiatric disorders and intellectual functioning throughout development in velocardiofacial (22q11.2 deletion) syndrome. *J. Am. Acad. Child Adolesc. Psychiatry* 48, 1060–1068.
- Hart, S.J., Davenport, M.L., Hooper, S.R., Belger, A., 2006. Visuospatial executive function in Turner syndrome: functional MRI and neurocognitive findings. *Brain* 129, 1125–1136.
- Held, K.R., et al., 1992. Mosaicism in 45,X Turner syndrome: does survival in early pregnancy depend on the presence of two sex chromosomes? *Brain* 88 (3), 288–294.
- Hoeft, F., Barnea-Goraly, N., Haas, B.W., Golarai, G., Ng, D., Mills, D., Korenberg, J., Bellugi, U., Galaburda, A., Reiss, A.L., 2007a. More is not always better: increased fractional anisotropy of superior longitudinal fasciculus associated with poor visuospatial abilities in Williams syndrome. *J. Neurosci.* 27, 11960–11965.
- Hoeft, F., Hernandez, A., Parthasarathy, S., Watson, C.L., Hall, S.S., Reiss, A.L., 2007b. Frontostriatal dysfunction and potential compensatory mechanisms in male adolescents with Fragile X syndrome. *Hum. Brain Mapp.* 28, 543–554.
- Holsen, L.M., Dalton, K.M., Johnstone, T., Davidson, R.J., 2008. Prefrontal social cognition network dysfunction underlying face encoding and social anxiety in Fragile X syndrome. *Neuroimage* 43, 592–604.
- Holzäpfel, M., Barnea-Goraly, N., Eckert, M.A., Kesler, S.R., Reiss, A.L., 2006. Selective alterations of white matter associated with visuospatial and sensorimotor dysfunction in Turner syndrome. *J. Neurosci.* 26, 7007–7013.
- Hubbard, E.M., Piazza, M., Pinel, P., Dehaene, S., 2005. Interactions between number and space in parietal cortex. *Nat. Rev. Neurosci.* 6, 435–448.
- Iglesias, J.E., Cheng-Yi, L., Thompson, P.M., Zhuowen, T., 2011. Robust brain extraction across datasets and comparison with publicly available methods. *IEEE Trans. Med. Imaging* 30, 1617–1634.
- Irwin, S.A., Galvez, R., Greenough, W.T., 2000. Dendritic spine structural anomalies in Fragile-x mental retardation syndrome. *Cereb. Cortex* 10, 1038–1044.
- Jenkinson, M., Smith, S., 2001. A global optimisation method for robust affine registration of brain images. *Med. Image Anal.* 5, 143–156.
- Karayiorgou, M., Simon, T.J., Gogos, J.A., 2010. 22q11.2 microdeletions: linking DNA structural variation to brain dysfunction and schizophrenia. *Nat. Rev. Neurosci.* 11, 402–416.
- Kates, W.R., Abrams, M.T., Kaufmann, W.E., Breiter, S.N., Reiss, A.L., 1997. Reliability and validity of MRI measurement of the amygdala and hippocampus in children with Fragile X syndrome. *Psychiatry Res.* 75, 31–48.
- Kates, W.R., Burnette, C.P., Jabs, E.W., Rutberg, J., Murphy, A.M., Grados, M., Geraghty, M., Kaufmann, W.E., Pearlson, G.D., 2001. Regional cortical white matter reductions

- in velocardiofacial syndrome: a volumetric MRI analysis. *Biol. Psychiatry* 49, 677–684.
- Kesler, S.R., Blasey, C.M., Brown, W.E., Yankowitz, J., Zeng, S.M., Bender, B.G., Reiss, A.L., 2003. Effects of X-monosomy and X-linked imprinting on superior temporal gyrus morphology in Turner syndrome. *Biol. Psychiatry* 54, 636–646.
- Kesler, S.R., Haberecht, M.F., Menon, V., Warsofsky, I.S., Dyer-Friedman, J., Neely, E.K., Reiss, A.L., 2004. Functional neuroanatomy of spatial orientation processing in Turner syndrome. *Cereb. Cortex* 14, 174–180.
- Kiehl, T.R., Chow, E.W., Mikulis, D.J., George, S.R., Bassett, A.S., 2009. Neuropathologic features in adults with 22q11.2 deletion syndrome. *Cereb. Cortex* 19, 153–164.
- Kogan, C.S., Bertone, A., Cornish, K., Boutet, I., Der Kaloustian, V.M., Andermann, E., Faubert, J., Chaudhuri, A., 2004. Integrative cortical dysfunction and pervasive motion perception deficit in Fragile X syndrome. *Neurology* 63, 1634–1639.
- Lebel, C., Walker, L., Leemans, A., Phillips, L., Beaulieu, C., 2008. Microstructural maturation of the human brain from childhood to adulthood. *Neuroimage* 40, 1044–1055.
- Lee, A.D., Leow, A.D., Lu, A., Reiss, A.L., Hall, S., Chiang, M.-C., Toga, A.W., Thompson, P.M., 2007. 3D pattern of brain abnormalities in Fragile X syndrome visualized using tensor-based morphometry. *Neuroimage* 34, 924–938.
- Lee, J.E., Chung, M.K., Lazar, M., DuBray, M.B., Kim, J., Bigler, E.D., Lainhart, J.E., Alexander, A.L., 2009. A study of diffusion tensor imaging by tissue-specific, smoothing-compensated voxel-based analysis. *Neuroimage* 44 (3), 870–883.
- Leow, A., Huang, S.-C., Geng, A., Becker, J., Davis, S., Toga, A., Thompson, P., 2005. Inverse consistent mapping in 3D deformable image registration: its construction and statistical properties. In: Christensen, G.E., Sonka, M. (Eds.), *Inf. Process. Med. Imaging*, vol. 3565. Springer, Berlin/Heidelberg, pp. 493–503.
- Leow, A.D., Yanovsky, I., Ming-Chang, C., Lee, A.D., Klunder, A.D., Lu, A., Becker, J.T., Davis, S.W., Toga, A.W., Thompson, P.M., 2007. Statistical properties of Jacobian maps and the realization of unbiased large-deformation nonlinear image registration. *IEEE Trans. Med. Imaging* 26, 822–832.
- Lippe, B., 1991. Turner syndrome. *Endocrinol. Metab. Clin. North Am.* 20, 121–152.
- Machado, A.M., Simon, T.J., Nguyen, V., McDonald-McGinn, D.M., Zackai, E.H., Gee, J.C., 2007. Corpus callosum morphology and ventricular size in chromosome 22q11.2 deletion syndrome. *Brain Res.* 1131, 197–210.
- Mazzocco, M.M., Bhatia, N.S., Lesniak-Karpiak, K., 2006. Visuospatial skills and their association with math performance in girls with Fragile X or Turner syndrome. *Child Neuropsychol.* 12, 87–110.
- Meechan, D.W., Tucker, E.S., Maynard, T.M., LaMantia, A.S., 2009. Diminished dosage of 22q11 genes disrupts neurogenesis and cortical development in a mouse model of 22q11 deletion/DiGeorge syndrome. *Proc. Natl. Acad. Sci. U. S. A.* 106, 16434–16445.
- Menon, V., Leroux, J., White, C., Reiss, A., 2004. Frontostriatal deficits in Fragile X syndrome: relation to FMR1 gene expression. *Proc. Natl. Acad. Sci. U. S. A.* 101, 3615.
- Molko, N., Cachia, A., Riviere, D., J-Fo, Mangin, Bruandet, M., Le Bihan, D., Cohen, L., Dehaene, S., 2003. Functional and structural alterations of the intraparietal sulcus in a developmental dyscalculia of genetic origin. *Neuron* 40, 847–858.
- Molko, N., Cachia, A., Riviere, D., Mangin, J.F., Bruandet, M., LeBihan, D., Cohen, L., Dehaene, S., 2004. Brain anatomy in Turner syndrome: evidence for impaired social and spatial-numerical networks. *Cereb. Cortex* 14, 840–850.
- Murphy, D.G., DeCarli, C., Daly, E., Haxby, J.V., Allen, G., White, B.J., McIntosh, A.R., Powell, C.M., Horwitz, B., Rapoport, S.I., et al., 1993. X-chromosome effects on female brain: a magnetic resonance imaging study of Turner's syndrome. *Lancet* 342, 1197–1200.
- Murphy, M.M., Mazzocco, M.M.M., Gerner, G., Henry, A.E., 2006. Mathematics learning disability in girls with Turner syndrome or Fragile X syndrome. *Brain Cogn.* 61, 195–210.
- Nilsson, K.O., Albertsson-Wikland, K., Alm, J., Aronson, S., Gustafsson, J., Hagenas, L., Hager, A., Ivarsson, S.A., Karlberg, J., Kristrom, B., Marcus, C., Moell, C., Ritzén, M., Tuvemo, T., Wattsgard, C., Westgren, U., Westphal, O., Aman, J., 1996. Improved final height in girls with Turner's syndrome treated with growth hormone and oxandrolone. *J. Clin. Endocrinol. Metab.* 81, 635–640.
- Oberle, I., Rousseau, F., Heitz, D., Kretz, C., Devys, D., Hanauer, A., Boue, J., Bertheas, M., Mandel, J., 1991. Instability of a 550-base pair DNA segment and abnormal methylation in Fragile X syndrome. *Science* 252, 1097–1102.
- Palo, J., Savolainen, H., 1973. The proteins of human myelin in inborn errors of metabolism and in chromosomal anomalies. *Acta Neuropathol.* 24, 56–61.
- Qiu, D., Tan, L.-H., Zhou, K., Khong, P.-L., 2008. Diffusion tensor imaging of normal white matter maturation from late childhood to young adulthood: voxel-wise evaluation of mean diffusivity, fractional anisotropy, radial and axial diffusivities, and correlation with reading development. *Neuroimage* 41, 223–232.
- Reiss, A.L., Dant, C.C., 2003. The behavioral neurogenetics of Fragile X syndrome: analyzing gene–brain–behavior relationships in child developmental psychopathologies. *Dev. Psychopathol.* 15, 927–968.
- Reiss, A.L., Abrams, M.T., Greenlaw, R., Freund, L., Denckla, M.B., 1995a. Neurodevelopmental effects of the FMR-1 full mutation in humans. *Nat. Med.* 1, 159–167.
- Reiss, A.L., Mazzocco, M.M., Greenlaw, R., Freund, L.S., Ross, J.L., 1995b. Neurodevelopmental effects of X monosomy: a volumetric imaging study. *Ann. Neurol.* 38, 731–738.
- Rivera, S.M., Menon, V., White, C.D., Glaser, B., Reiss, A.L., 2002. Functional brain activation during arithmetic processing in females with Fragile X syndrome is related to FMR1 protein expression. *Hum. Brain Mapp.* 16, 206–218.
- Robin, N.H., Taylor, C.J., McDonald-McGinn, D.M., Zackai, E.H., Bingham, P., Collins, K.J., Earl, D., Gill, D., Granata, T., Guerrini, R., Katz, N., Kimonis, V., Lin, J.P., Lynch, D.R., Mohammed, S.N., Massey, R.F., McDonald, M., Rogers, R.C., Split, M., Stevens, C.A., Tischkowitz, M.D., Stoodley, N., Leventer, R.J., Pilz, D.T., Dobyns, W.B., 2006. Polymicrogyria and deletion 22q11.2 syndrome: window to the etiology of a common cortical malformation. *Am. J. Med. Genet. A* 140, 2416–2425.
- Romans, S.M., Stefanatos, G., Roeltgen, D.P., Kushner, H., Ross, J.L., 1998. Transition to young adulthood in Ullrich–Turner syndrome: neurodevelopmental changes. *Am. J. Med. Genet.* 79, 140–147.
- Ross, J., Stefanatos, G., Kushner, H., Zinn, A., Bondy, C., Roeltgen, D., 2002. Persistent cognitive deficits in adult women with Turner syndrome. *Neurology* 58, 218–225.
- Ross, J., Zinn, A., McCauley, E., 2000. Neurodevelopmental and psychosocial aspects of Turner syndrome. *Ment. Retard. Dev. Disabil. Res. Rev.* 6, 135–141.
- Rovet, J., Netley, C., 1980. The mental rotation task performance of Turner syndrome subjects. *Behav. Genet.* 10 (5), 437–443.
- Rovet, J., Ireland, L., 1994. Behavioral Phenotype in Children with Turner Syndrome. *J. Psychiatr. Psychol.* 19 (6), 779–790.
- Rudelli, R.D., Brown, W.T., Wisniewski, K., Jenkins, E.C., Laure-Kamionowska, M., Connell, F., Wisniewski, H.M., 1985. Adult Fragile X syndrome. *Acta Neuropathol.* 67, 289–295.
- Scerif, G., Cornish, K., Wilding, J., Driver, J., Karmiloff-Smith, A., 2004. Visual search in typically developing toddlers and toddlers with Fragile X or Williams syndrome. *Dev. Sci.* 7, 116–130.
- Scerif, G., Cornish, K., Wilding, J., Driver, J., Karmiloff-Smith, A., 2007. Delineation of early attentional control difficulties in Fragile X syndrome: focus on neurocomputational changes. *Neuropsychologia* 45, 1889–1898.
- Schaer, M., Eric Schmitt, J., Glaser, B., Fo, Lazeyras, Delavelle, J., Eliez, S., 2006. Abnormal patterns of cortical gyrification in velo-cardio-facial syndrome (deletion 22q11.2): an MRI study. *Psychiatry Res. Neuroimaging* 146, 1–11.
- Shashi, V., Muddasani, S., Santos, C.C., Berry, M.N., Kwapiil, T.R., Lewandowski, E., Keshavan, M.S., 2004. Abnormalities of the corpus callosum in nonpsychotic children with chromosome 22q11 deletion syndrome. *Neuroimage* 21, 1399–1406.
- Silbert, A., Wolff, P.H., Lilienthal, J., 1977. Spatial and temporal processing in patients with Turner's syndrome. *Behav. Genet.* 7 (1), 11–21.
- Simon, T.J., 1997. Reconceptualizing the origins of number knowledge: a “non-numerical” account. *Cogn. Dev.* 12, 349–372.
- Simon, T.J., 2007. Cognitive characteristics of children with genetic syndromes. *Child Adolesc. Psychiatr. Clin. N. Am.* 16, 599–616.
- Simon, T.J., 2011. Clues to the foundations of numerical cognitive impairments: evidence from genetic disorders. *Dev. Neuropsychol.* 36, 788–805.
- Simon, T.J., Bearden, C.E., Mc-Ginn, D.M., Zackai, E., 2005a. Visuospatial and numerical cognitive deficits in children with chromosome 22q11.2 deletion syndrome. *Cortex* 41, 145–155.
- Simon, T.J., Ding, L., Bish, J.P., McDonald-McGinn, D.M., Zackai, E.H., Gee, J., 2005b. Volumetric, connective, and morphologic changes in the brains of children with chromosome 22q11.2 deletion syndrome: an integrative study. *Neuroimage* 25, 169–180.
- Simon, T.J., Takarae, Y., DeBoer, T., McDonald-McGinn, D.M., Zackai, E.H., Ross, J.L., 2008a. Overlapping numerical cognition impairments in children with chromosome 22q11.2 deletion or Turner syndromes. *Neuropsychologia* 46, 82–94.
- Simon, T.J., Wu, Z., Avants, B., Zhang, H., Gee, J.C., Stebbins, G.T., 2008b. Atypical cortical connectivity and visuospatial cognitive impairments are related in children with chromosome 22q11.2 deletion syndrome. *Behav. Brain Funct.* 4, 25.
- Smith, S.M., 2002. Fast robust automated brain extraction. *Hum. Brain Mapp.* 17, 143–155.
- Smith, S.M., Jenkinson, M., Johansen-Berg, H., Rueckert, D., Nichols, T.E., Mackay, C.E., Watkins, K.E., Ciccarelli, O., Cader, M.Z., Matthews, P.M., Behrens, T.E.J., 2006. Tractbased spatial statistics: voxelwise analysis of multisubject diffusion data. *Neuroimage* 31, 1487–1505.
- Stoddard, J., Niendam, T., Hendren, R., Carter, C., Simon, T.J., 2010. Attenuated positive symptoms of psychosis in adolescents with chromosome 22q11.2 deletion syndrome. *Schizophr. Res.* 118, 118–121.
- Sy, J., Alturkustani, M., Ang, L.-C., 2010. Intracallosal longitudinal fiber bundle: an unexpected finding mimicking demyelination in a patient with Turner syndrome. *Acta Neuropathol.* 120, 545–547.
- Sztriha, L., Guerrini, R., Harding, B., Stewart, F., Chelloug, N., Johansen, J.G., 2004. Clinical, MRI, and pathological features of polymicrogyria in chromosome 22q11 deletion syndrome. *Am. J. Med. Genet. A* 127A, 313–317.
- Temple, C.M., Carney, R.A., 1995. Patterns of spatial functioning in Turner's syndrome. *Cortex* 31 (1), 109–118.
- Terao, Y., Hashimoto, K., Nukina, N., Mannen, T., Shinohara, T., 1996. Cortical dysgenesis in a patient with Turner mosaicism. *Dev. Med. Child Neurol.* 38, 455–460.
- Thomason, M.E., Thompson, P.M., 2011. Diffusion imaging, white matter, and psychopathology. *Annu. Rev. Clin. Psychol.* 7, 63–85.
- Tombini, M., Marciani, M.G., Romigi, A., Izzi, F., Sperli, F., Zozzo, A., Floris, R., De Simone, R., Placidi, F., 2003. Bilateral frontal polymicrogyria and epilepsy in a patient with Turner mosaicism: a case report. *J. Neurol. Sci.* 213, 83–86.
- Tournier, J.-D., Mori, S., Leemans, A., 2011. Diffusion tensor imaging and beyond. *Magn. Reson. Med.* 65, 1532–1556.
- van Amelsvoort, T., Daly, E., Robertson, D., Suckling, J., Ng, V., Critchley, H., Owen, M.J., Henry, J., Murphy, K.C., Murphy, D.G., 2001. Structural brain abnormalities associated with deletion at chromosome 22q11: quantitative neuroimaging study of adults with velo-cardio-facial syndrome. *Br. J. Psychiatry* 178, 412–419.
- van Amelsvoort, T., Schmitz, N., Daly, E., Deeley, Q., Critchley, H., Henry, J., Robertson, D., Owen, M., Murphy, K.C., Murphy, D.G., 2006. Processing facial emotions in adults with velo-cardio-facial syndrome: functional magnetic resonance imaging. *Br. J. Psychiatry* 189, 560–561.
- van Eimeren, L., Grabner, R.H., Koschutnig, K., Reishofer, G., Ebner, F., Ansari, D., 2010. Structure–function relationships underlying calculation: a combined diffusion tensor imaging and fMRI study. *Neuroimage* 52, 358–363.
- Verkerk, A.J.M.H., Pieretti, M., Sutcliffe, J.S., Fu, Y.-H., Kuhl, D.P.A., Pizzuti, A., Reiner, O., Richards, S., Victoria, M.F., Zhang, F., Eussen, B.E., van Ommen, G.-J.B., Blonden, L.A.J., Riggins, G.J., Chastain, J.L., Kunst, C.B., Galjaard, H., Thomas Caskey, C., Nelson, D.L.,

- Oostra, B.A., Warren, S.T., 1991. Identification of a gene (FMR-1) containing a CCG repeat coincident with a breakpoint cluster region exhibiting length variation in Fragile X syndrome. *Cell* 65, 905–914.
- Vestergaard, M., Madsen, K.S., Baar√©, W.F.C., Skimminge, A., Ejersbo, L.R., Rams√©y, T.Z., Gerlach, C., √©keson, P., Paulson, O.B., Jernigan, T.L., 2010. White matter microstructure in superior longitudinal fasciculus associated with spatial working memory performance in children. *J. Cogn. Neurosci.* 23, 2135–2146.
- Walsh, V., 2003. A theory of magnitude: common cortical metrics of time, space and quantity. *Trends Cogn. Sci.* 7, 483–488.
- Walter, E., Mazaika, P.K., Reiss, A.L., 2009. Insights into brain development from neurogenetic syndromes: evidence from Fragile X syndrome, Williams syndrome, Turner syndrome and velocardiofacial syndrome. *Neuroscience* 164, 257–271.
- Wang, P.P., Woodin, M.F., Kreps-Falk, R., Moss, E.M., 2000. Research on behavioral phenotypes: velocardiofacial syndrome (deletion 22q11.2). *Dev. Med. Child Neurol.* 42, 422–427.
- Wisniewski, K.E., Segan, S.M., Mizejeski, C.M., Sersen, E.A., Rudelli, R.D., 1991. The fra(X) syndrome: neurological, electrophysiological, and neuropathological abnormalities. *Am. J. Med. Genet.* 38, 476–480.
- Woods, R.P., Grafton, S.T., Watson, J.D.G., Sicotte, N.L., Mazziotta, J.C., 1998. Automated image registration: II. Intersubject validation of linear and nonlinear models. *J. Comput. Assist. Tomogr.* 22, 153–165.
- Yamagata, B., Barnea-Goraly, N., Marzelli, M.J., Park, Y., Hong, D.S., Mimura, M., Reiss, A.L., 2011. White Matter Aberrations in Prepubertal EstrogenNaive Girls with Monosomic Turner Syndrome. *Cereb. Cortex.*